J Solid State Electrochem (2007) 11:496–504
DOI 10.1007/s10008-006-0186-z

ORIGINAL PAPER

Electrochemical and microscopic studies of surface-confined DNA

Xiaoquan Lu · Yan Zhang · Min Zhang · Yina Chen · Jingwan Kang

Received: 28 April 2006 / Revised: 10 May 2006 / Accepted: 14 June 2006 / Published online: 26 August 2006

Abstract We have studied the micropatterning and characterization of the organic monolayers using cyclic voltammetry (CV), scanning electrochemical microscopy (SECM), atom force microscopy, and AC impedance, and have determined the electrochemical parameters, i.e., the apparent reaction rate constant (K_f) and the coverage of the electrode surface (θ). CV and SECM experiments demonstrated that the surface of the modified electrode represents an insulating substrate for ferricyanide. Using the high sensitivity of the electron transfer of ferricyanide to the modification of the gold surface with DNA, we selected this reaction as a probe to study the different modification stages at this modified electrode. SECM images obtained from bare, partially modified, and totally modified electrodes showed very good resolution with different topographies or null according to the extent of modification. Based on a comparison with the results of the experiments, a reasonable agreement can be obtained, which means a conjunction of these techniques.

Keywords Calf thymus DNA · Self-assembled monolayer (SAM) · Scanning electrochemical microscope (SECM) · Atom force microscope (AFM) · Electrochemistry

Introduction

The development of techniques for characterization and micropatterning biomolecules on solid substrates is of major importance for analytical applications in electroanalytical procedures, for sensor development, for electrochemical technology, and for fundamental electrochemistry. DNA-modified electrodes have been applied for analytical purposes over the past few decades [1]. They are crucially important for developing electrochemical DNA biosensors [2] and for studying the interactions of DNA with other molecules [3, 4]. Electrochemical measurements have long been used to characterize modified electrodes, whether the modification is a polymer coating or a self-assembled monolayer (SAM). Electrodes modified with DNA have been electrochemically characterized as well. Compared with the conventional electrochemical methods, many relevant techniques have been developed to study the immobilization of calf thymus DNA molecules on the gold surfaces, such as scanning tunneling microscopy, atomic force microscopy (AFM), and scanning electrochemical microscopy (SECM) [5–8]. Among these methods, SECM has been shown to be particularly promising for microfabrication [9–12] in studies of immobilized biomolecules and chemical or biological reactions at the electrode/solution interface [13–15]. Additionally, one of the applications of the SECM techniques is the use of the ultramicroelectrode (UME) tip to obtain images of different substrate surfaces. It can be used to distinguish regions of different conductivity or electrochemical activity at high resolution. In addition to its imaging capabilities, SECM is an electrochemical tool that can be used to study electrode reactions and homogeneous reactions of tip-generated species that occur in the small gap between the tip and the substrate. Two different modes of operation, i.e., the direct [5, 6] and feedback modes [10–12], have been used to obtain images of microstructures of biologically active surfaces with high spatial resolution, to determine rate constants of surface reactions, and to study electron transfer (ET) on the interface.

SAMs comprising hydrocarbons bound to a gold surface via a S–Au linkage are the most widely studied systems for

X. Lu (✉) · Y. Zhang · M. Zhang · Y. Chen · J. Kang
Department of Chemistry, Northwest Normal University, Lanzhou 730070, Gansu, People's Republic of China
e-mail: luxq@nwnu.edu.cn

the understanding of the fundamental properties of SAMs. Based on the results, the covalent attachment of functional molecules to the terminal of SAMs has been pursued to construct well-organized molecular assemblies containing photo- and/or electroactive molecules on gold electrodes. Reported here is the immobilization of DNA onto the gold electrode surface through a self-assembly method, by which very stable DNA-modified electrodes can be obtained. The SAM/Au with a DNA-modified electrode was characterized by means of cyclic voltammetry (CV), SECM, AFM, and AC impedance methods using a redox couple as a probe. The modification of gold electrodes with DNA is a known matter, and SECM analysis of this modified surface was studied previously and we have focused our study on the DNA modification process. In particular, the influences of the adsorption time and the preconditioning potential on the gold surface will be examined. With the SECM experiments, we hope to find an electrochemical microscopic view of the layer that is impossible to obtain with conventional techniques. Moreover, AFM and AC impedance methods can well be utilized to prove the result of the SECM.

Experimental procedures

Reagents

Calf thymus DNA obtained from Huamei (Shanghai, People's Republic of China) was used as received. Solutions of DNA (ca. 10^{-5} mol·L^{-1} in nucleotide phosphate) in 50 mM NaCl/5 mM Tris pH 7.10 gave a ratio of UV absorbance at 260–280 nm, A_{260}/A_{280} of ca.1.7–1.8, indicating that the DNA could be used [16, 17]. The supporting electrolyte for all experiments was 0.1 mol·L^{-1} Tris–HCl buffer (pH 6). All solutions were deoxygenated via purging with N_2 for 15 min prior to each measurement. Other chemicals were of analytical reagent grade. Water was double distilled.

CV measurements

The CV experiment was carried out with a CHI 660 electrochemical workstation (CH Instrument, Austin, TX, USA) in a one-compartment, three-electrode system at a room temperature of 25±2 °C. A bare gold electrode or dsDNA–SAM/Au was used as the working electrode (CH Instrument). An Ag/AgCl electrode was used as a reference electrode and a platinum wire served as the counter electrode.

Immobilization of dsDNA on SAMs on gold electrode

A gold disk electrode was polished first with emery paper followed by alumina paste (Maruto, Tokyo, Japan; 1.0, 0.3, and 0.05) and then rinsed ultrasonically with twice-distilled water. After being cleaned ultrasonically in a bath containing ethanol and acetone sequentially, the gold electrode was chemically etched by dipping in conc. 98% H_2SO_4–28% H_2O_2 (3:1 vol) for 10 min to oxidize any impurities, which was followed by rinsing with twice-distilled water. The gold electrode was then etched electrochemically by scanning the electrode in 1 M H_2SO_4 (+1.2 to −0.2 V) vs Ag/AgCl until the characteristic for the clean gold electrode was obtained. After being rinsed by twice-distilled water and dried by an infrared lamp, the gold electrode was immersed in the acetone solution containing 1 mM thioglycolic acid and 1.0×10^{-3} M DNA. Finally, the modified gold electrode was left in the stirred solution for 48 h and then ultrasonically treated in twice-distilled water, ethanol, and acetone successively before the measurement. Thus, the SAM/Au modified electrode with DNA was obtained (Scheme 1).

SECM apparatus

All SECM experiments were carried out with a CHI 900 setup (CH Instrument). A 25-μm-diameter Pt UME was employed as the SECM tip. The tip was fabricated as described previously [18]. Before each measurement, the electrode was polished with emery paper followed by

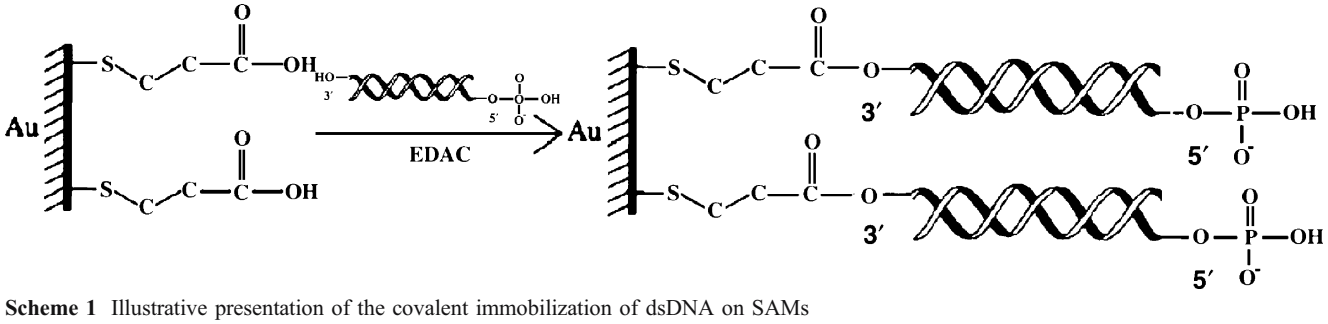

Scheme 1 Illustrative presentation of the covalent immobilization of dsDNA on SAMs

diamond paste (from 6 to 1 nm) on a nylon polishing cloth and 0.05-μm alumina. An Ag/AgCl electrode in saturated KCl and a Pt wire were used as reference and counter electrodes, respectively. Here, the DNA-modified and bare electrodes were used as the substrate. Before each experiment, the bare Au substrate was polished with 0.05-μm alumina, and then rinsed with twice-distilled water.

The UME was biased at −0.2 V in the solution of 1 mmol·L^{-1} $Fe(CN)_6^{3-}$ and 50 mmol·L^{-1} KCl, and the substrate was biased at +0.6 V. So, the Pt UME was withdrawn and the feedback current was recorded under the above condition. The SECM image of the gold dots was obtained by scanning the Pt UME (25 μm in diameter, 0.6 V vs Ag/AgCl) laterally with a speed of 1 μm·s^{-1} in the solution of 1 mmol·L^{-1} of $Fe(CN)_6^{3-}$ and 50 mmol·L^{-1} KCl. The potential of the UME was set at −0.2 V to ensure the diffusion-controlled reduction of $Fe(CN)_6^{3-}$. All experiments were carried out at a room temperature of 25±2 °C.

AC impedance

AC impedance measurements were performed with a CHI 660 electrochemical workstation (CH Instrument) in a one-compartment, three-electrode system at a room temperature of 25±2 °C. The potential was controlled at the open-circuit value, and the frequency was varied over the range 10^5–1 Hz, with an amplitude of 5 mV. Either a bare gold electrode or dsDNA–SAM/Au was used as the working electrode (CH Instrument). An Ag/AgCl electrode was used as a reference electrode and a platinum wire served as the counter electrode.

Results and discussion

Modification of the gold electrode with thioglycolic acid and determination of surface coverage of S–Au SAM films

The Au electrode is modified according to the procedure described previously [19]. The thioglycolic acid is covalently bound to the gold surface via the chemisorption of thiol groups to gold. As evidence of the strong chemical interaction between thiol and gold, the surface coverage (Γ) of SAM-forming molecules can be estimated by the CV. The electrochemical reductive desorption of SAMs from Au electrodes exhibits a peak at about −0.968 V by scanning from −0.4 to −1.2 V in a 0.5-M KOH aqueous solution (Fig. 1). The peak is produced by the reductive desorption of thiolate compound chemisorbed to Au. It shows that the thiolate compound was adsorbed on the Au electrode and is desorbed. The corresponding process and

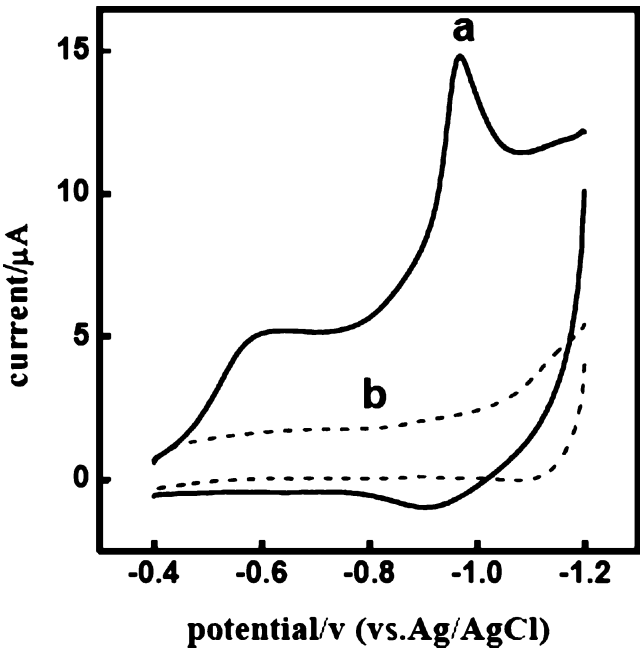

Fig. 1 Voltammetric response of reductive desorption of SAM film in a 0.5-M KOH (*a*) compared to bare Au electrode (*b*); scan rate=0.1 V s^{-1}

reaction mechanism [20] are shown as the following equation:

$$R\text{-}S\text{-}Au + e^- = Au^0 + R\text{-}S^- \quad (1)$$

The surface coverage (Γ) is calculated to be 3.18×10^{-10} mol/cm^2 by integrating charges (Q) passing on reduction peak at 100 mV/s. According to the following equation:

$$\Gamma = Q/nFA \quad (2)$$

where A is the electrode surface area, F is Faraday's constant, and n is the number of electrons involved in the electrode reaction [21]. On the other hand, from the AFM image of the SAM film, there is good agreement with the formation of the carboxyl-terminated SAM.

Surface analysis

The covalent immobilization of DNA on a SAM/Au surface by self-assembly method is illustrated in Scheme 1 [22]. Modification of gold surface with thiol-terminated DNA is characterized by CV, and the redox behavior of a reversible couple, $Fe(CN)_6^{3-} / Fe(CN)_6^{4-}$, can be used to probe the packing structure of the monolayer. Figure 2 shows the cyclic voltammograms of the bare (curve a), SAM/Au (curve b), and DNA-modified SAM/Au (curve c) electrodes in 1 mM $K_3Fe(CN)_6$ solution. Comparing Fig. 2 curve a

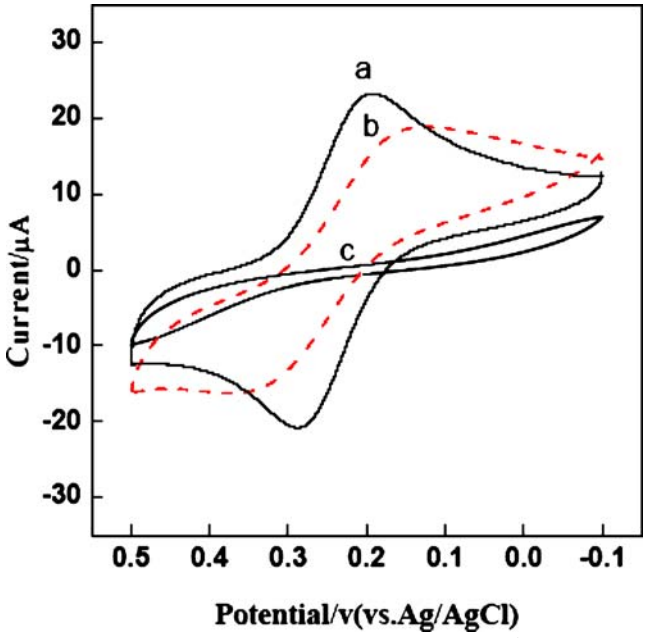

Fig. 2 Cyclic voltammograms for the 1-mmol·L^{-1} $K_3Fe(CN)_6$ solution in 0.1 M Tris–HCl buffer (pH 6.0) obtained (*a*) at the bare gold electrode, (*b*) at the SAM/Au electrode, and (*c*) at the dsDNA-modified SAM/Au electrode at a scan rate of 0.1 V s^{-1}

with curves b and c, it can be seen that the CV curve of $Fe(CN)_6^{3-}$ at the bare electrode displayed features characteristic of a reversible process (the peak separation ΔE=70 mV). However, from Fig. 2 (curve b), the current for the $Fe(CN)_6^{3-}$ decreased in comparison with those of curve a, and the potential shifted negatively by 80 mV at the SAM/Au electrode (curve b), indicating the formation of the carboxyl-terminated SAM. On the other hand, the redox waves were completely irreversible for the $Fe(CN)_6^{3-}$ at the DNA-modified SAM/Au electrode and the potentials are shifted more negative by 182 mV compared to those at the bare and SAM/Au surfaces. This difference is likely a consequence of the decreased dielectric constant in the diffuse monolayer compared with that of the bulk solution and increased electrostatic repulsion between $Fe(CN)_6^{3-}$ and deoxyribose-phosphate of the dsDNA. So, it has been pointed out that DNA assembled on the electrode surface are densely packed and well organized and act as an effective electron and ion barrier to inhibit the transport of species, which will make the ET of the indicator slower at the DNA-modified SAM/Au electrode than at the bare gold electrode. Consequently, the access of $Fe(CN)_6^{3-}$ to the gold electrode is efficiently inhibited by the film, and it causes a complete inhibition of ET in the reduction peak current.

As $Fe(CN)_6^{3-}$ does not bind to the DNA polyanion, the decrease of the peak current at the modified electrode implies essentially complete coverage by the thiol-terminated DNA. In summary, the characteristics of the surface changes indicate that DNA can be well immobilized onto the gold electrode surface. To ensure that $Fe(CN)_6^{3-}$ is not merely electrostatically repelled from holes in the monolayer, a neutral probe, ferrocene carboxaldehyde, is investigated under the same conditions and bears a similar result.

Surface coverage and reductive desorption of SAM/Au DNA from the gold electrode

Taking advantage that ET of ferricyanide is highly sensitive to the coverage of the gold surface, we select this reaction as a probe to study the adsorption and desorption of DNA–SAM/Au at the gold electrode. Figure 3 shows cyclic voltammograms of ferricyanide at the gold electrode modified with DNA after different adsorption times. The modified gold electrode is rinsed exhaustively before each voltammogram to remove physisorbed molecules. From this figure, it can be seen that as the adsorption time increased, the coverage of the gold electrode increased and DNA film tended to form highly ordered structures on the gold electrode. The cyclic voltammograms of ferricyanide show two main changes as a consequence of the surface modification: first, a decrease in current, and second, a loss of reversibility of the couple. Probably, these changes reveal that both the DNA-modified electrode area available for the redox processes and the heterogeneous ET rate are smaller. According to the method previously described by

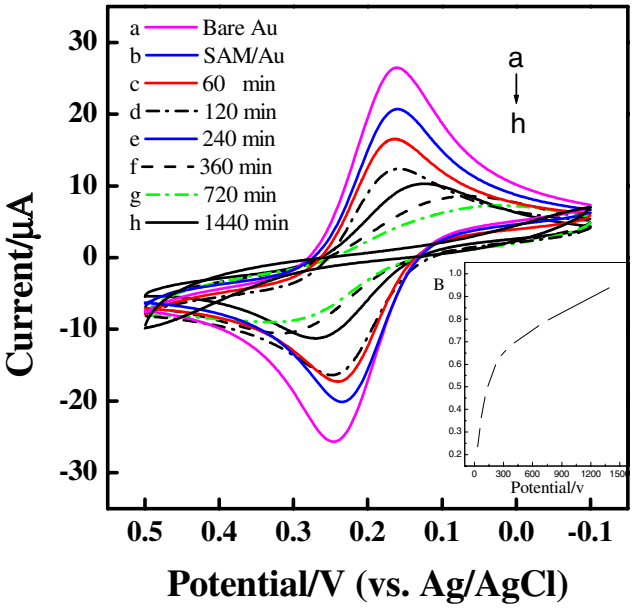

Fig. 3 Cyclic voltammograms of 1 mmol·L^{-1} ferricyanide in 0.1 M Tris–HCl buffer (pH 6.0) at a gold electrode modified at different adsorption times. Sweep rate=0.1 V s^{-1}. *Inset*: calculated hindrance *B* (Eq. 1) vs adsorption time. An overnight modification was considered as 24 h of modification (1,440 min)

Weisser et al. [23], we calculate the hindrance (B) of the electrode using the following equation:

$$B = 1 - \left[I_p^f(DNA - SAM/Au) \Big/ I_p^f(Au) \right] \quad (3)$$

Where $i_p^f(DNA - SAM/Au)$ and $i_p^f(Au)$ are the forward (reduction of ferricyanide) peak currents measured at both the modified and the bare electrodes, respectively. Then, B is a qualitative parameter for the layer density. The inset of Fig. 3 shows the dependence of hindrance of B with the adsorption time, revealing a gradual increase of the covering. After 1,440 min, a value of B=0.88 is reached, indicating practically a totally covered Au surface.

The DNA-modified layer formed on the gold surface is chemically stable, but there are two ways of removal, that is, mechanical polishing and electrochemical pretreatment. The covalent bond formed between Au and the −SH group is electrochemically reducible [24, 25] according to Eq. 1, too.

Figure 4 shows the cyclic voltammograms of ferricyanide at the DNA-modified gold electrode after different preconditioning potentials. We can observe that when the applied potential is more negative, the DNA-modified electrode suffers more desorption from the Au surface, as can be ascribed from the increased reduction of ferricyanide. The inset of Fig. 4 shows the dependence of hindrance B with the applied potential, revealing a gradual decrease of the covering when the preconditioning potentials were more negative, reaching B=0.25, and revealing a practically uncovered Au surface.

Furthermore, we also have used SECM to visualize the surface of gold electrochemically when this surface is bare or partially modified with DNA. Curves a–e in Fig. 5 are normalized current–distance curves recorded during the approach of the UME tip toward the bare and DNA-modified gold electrodes. For comparison, the current–distance curve acquired by bringing the tip close to a bare gold surface is presented as curve a. On the one hand, four approach curves done with the tip positioned at four different zones on the x–y surface of the partially modified electrode (B=0.34) are shown in Fig. 5 (curves b–e). On the other hand, the inset in Fig. 5 reveals cyclic voltammograms of ferricyanide obtained at the bare electrode (curve a) and at the partially modified electrode (B=0.34) (curve b). The corresponding SECM image is shown in Fig. 8b. These results show very well the difference of the microscopic approach obtained by SECM experiments from the macroscopic approach obtained by CV experiments. In the case of the CV measurements, we obtained only one CV curve for the partially modified electrode, but in the case of the SECM experiments, we obtained three different approach curves with different feedback currents depending on the tip position on the partially modified electrode surface. Furthermore, we can appreciate that the approach curves show different behaviors ranging from a totally positive

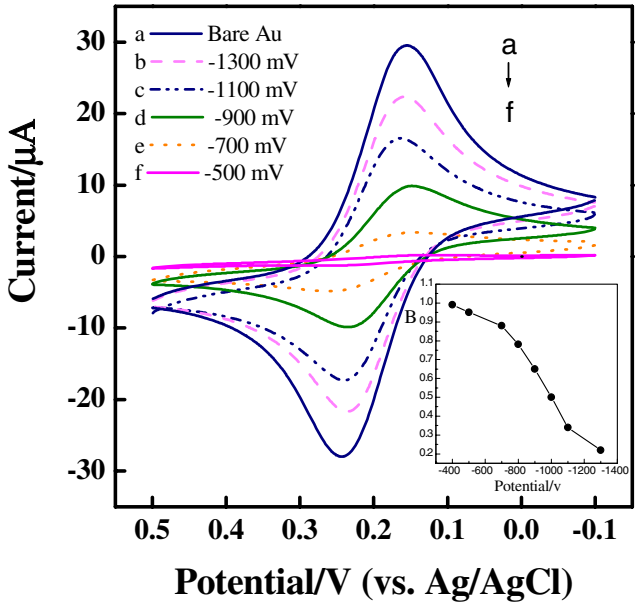

Fig. 4 Cyclic voltammograms of 1 mmol·L^{-1} ferricyanide in 0.1 M Tris–HCl buffer (pH 6.0) at a preconditioned modified DNA-modified gold electrode at different negative potentials for 40 s. Sweep rate=0.1 V s^{-1}. *Inset*: calculated hindrance B (Eq. 1) vs preconditioning potential

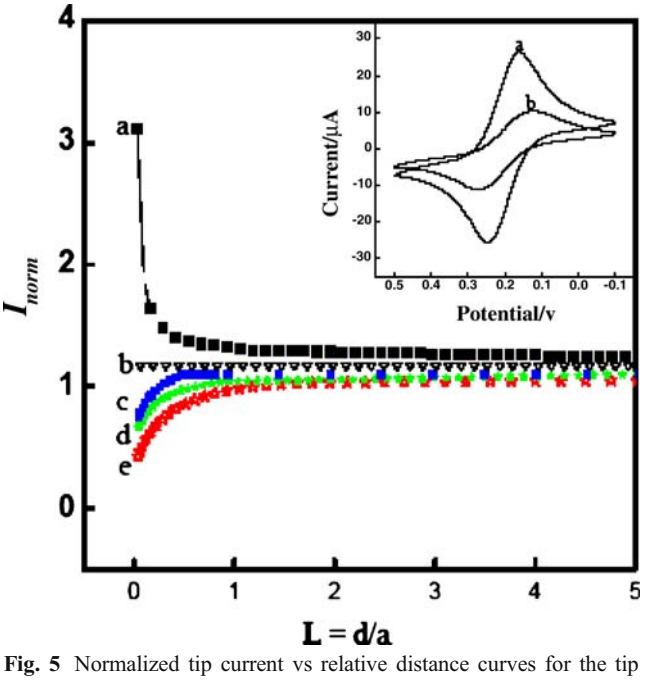

Fig. 5 Normalized tip current vs relative distance curves for the tip approaching the different zones of a partially DNA-modified gold electrode. System: 1 mmol·L^{-1} $K_3Fe(CN)_6$ in the buffer solution (pH 6.0), scan rate: 1 μm·s^{-1}. *Inset*: cyclic voltammograms of 1 mmol·L^{-1} ferricyanide in 0.1 M Tris–HCl buffer (pH 6.0) at bare (*curve a*) and partially modified DNA-modified (B=0.34, *curve b*) gold electrodes

(open pentacle Fig. 6 curve a) to a totally negative (open triangle Fig. 6 curve b) feedback current, but in the intermediate states the situation is rather different, showing a tip current increase and then decay, originating a peak-shaped response.

Electrochemical characterization of DNA–SAM/Au prepared from SAMs with SECM and AC impedance methods

The feedback mode is the main quantitative operation mode of SECM. When the tip is brought close (i.e., within a few tip radii) to a conductive substrate, the R species formed in tip reaction ($O+ne^- \rightarrow R$) diffuses to the substrate where it may be oxidized back to O ($R-ne^- \rightarrow O$). This process produces an additional flux of O to the tip, and hence, an increase in tip current $\left(i_T > i_{T,\infty}\right) \cdot i_{T,\infty}$, the steady-state current generated at the tip that is far from the substrate, is given by $i_{T,\infty} = 4nFDca$; F is Faraday's constant, n is the number of electrons transferred in the tip reaction, D is the diffusion coefficient of O, c is the bulk concentration of O, and a is the tip radius. This phenomenon is termed "positive feedback." On the contrary, if the substrate is an inert electrical insulator, the tip-generated species, R, cannot react on its surface. At small d, $i_T < i_{T,\infty}$, the negative feedback is observed.

The SECM technique can be employed to study the electrochemical performance of modified electrodes. In this case, the bare and DNA-modified electrodes can be used as substrates with a negatively charged mediator, $Fe(CN)_6^{3-}$. The principle behind the SECM feedback mode of surface-confined DNA molecules via $Fe(CN)_6^{3-}/Fe(CN)_6^{4-}$ can be illustrated by the following electrode reactions:

$$Fe(CN)_6^{3-} + e^- = Fe(CN)_6^{4-} \quad (4)$$

$$Fe(CN)_6^{4-} \quad e^- = Fe(CN)_6^{3-} \quad (5)$$

In a typical experiment, in the feedback mode employed here, the UME tip potential is held at a value of −0.2 V where a steady-state reduction of $Fe(CN)_6^{3-}$ occurs and the reduction is controlled by the diffusion of $Fe(CN)_6^{3-}$ (reaction 4). The product, $Fe(CN)_6^{4-}$, upon diffusion to the substrate surface and under the potential of 0.6 V, can be oxidized (reaction 5).

Curves a and b in Fig. 6 are normalized current–distance (I_T–L) curves recorded during the approach of the UME tip toward the bare and DNA-modified SAM/Au electrodes at a speed of 1 μm s^{-1}. Approach experiments carried out at the bare Au electrode (pentacle symbols) reveal a positive feedback between the Pt tip and the Au electrode in concordance with the theory of SECM approach curves. As the tip is close to the bare electrode, the oxidized species [$Fe(CN)_6^{3-}$] diffuse from the UME tip to the interface, and the mediator generated at the tip can undergo ET and be restored to its original oxidation state. This regeneration of the mediator in the gap between the tip and substrate causes the current to increase, producing a positive feedback. On the contrary, in the approach curves carried out at the modified electrode (triangle symbols), there is a negative feedback (Fig. 6 curve b), implying that the substrate (the DNA-modified electrode) acts as an insulating surface for ferricyanide, blocking diffusion of species from the tip, showing a decrease of the steady-state current. So, the concentration of $Fe(CN)_6^{3-}$ reduces between tip and substrate and i_T decreases at the same time. Such an abrupt transition from positive to negative feedback behavior can be attributed to the aforementioned depletion of reaction 5. Consequently, these SECM results agree very well with those obtained by CV, supporting that DNA forms an insulating film over the Au electrode for ferricyanide.

Figure 6 shows the experimental I_T–L curves fitted with the theoretical one [26]. It is found that a good agreement between theory (solid line) and experiment data (symbol) is obtained. The negative feedback proves that the surface-confined DNA is compact and can be covalently assembled on the Au electrode. In general, the changes that occurred at the electrode surface can be reflected by the AC impedance frequency spectrum. So, the AC impedance method can also be employed as an effective way to characterize the layers for the immobilization of DNA on SAM/Au.

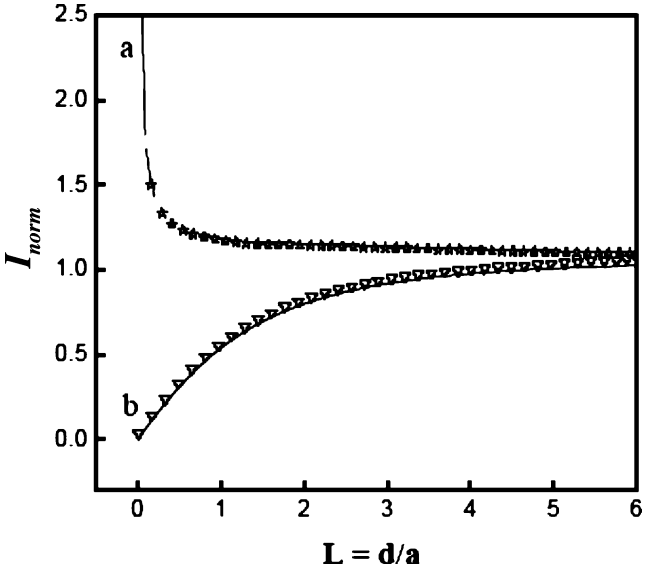

Fig. 6 Normalized tip current–distance curves for approaching the bare (*star*) and the DNA-modified SAM/Au (*open triangle*) electrodes fitted with theoretical curves over an insulating surface and a conductive surface, respectively (*line*). System: 1 mmol·L^{-1} $K_3Fe(CN)_6$ in the buffer solution (pH 6.0), scan rate: 1 μm·s^{-1}

Curve 1 and curve 2 in Fig. 7 show the complex plane AC impedance frequency spectrum (electrochemical impedance spectroscopy) at the bare and DNA-modified electrodes. As shown in Fig. 7, Z′ and Z″ represent the real and imaginary parts of the AC impedance frequency spectrum, respectively. For the bare gold electrode, a semicircle appears in the low-frequency region in the admittance spectrum and a straight line arises in the high-frequency region, as shown in Fig. 7 (curve 1). But, for the DNA–SAM/Au, as shown in Fig. 7 (curve 2), the larger semicircle in the high-frequency region at the DNA/Au can be observed, and the AC resistance R_{ct} is apparently larger than that at the bare electrode, which indicates that DNA assembled on the electrode surface blocks the ET between the indicator of $Fe(CN)_6^{3-}$ and the electrode surface [27]. $Fe(CN)_6^{4-} / Fe(CN)_6^{3-}$ cannot pass the holes in the self-assembled film to reach the electrode surface, and the gold surface is efficiently blocked by the film due to the low permeability of the film for highly charged ions and the low conductivity of the film as compared with the bare gold. Based on the results, it can be inferred that further evidence for uniform multilayer growth of DNA assemblies is obtained from AC impedance frequency spectrum.

According to the AC impedance frequency spectrum and these equations [28, 29] for the redox reactions 4 and 5, the AC resistance is

$$R_{ct} = \frac{RT}{nFi_0} \tag{6}$$

According to Eq. 6, the following relationship is derived:

$$i_0 = \frac{RT}{nFR_{ct}} \tag{7}$$

where R_{ct} is the AC resistance, n is the ET numbers, i_0 is AC current density, and F is Faraday's constant.

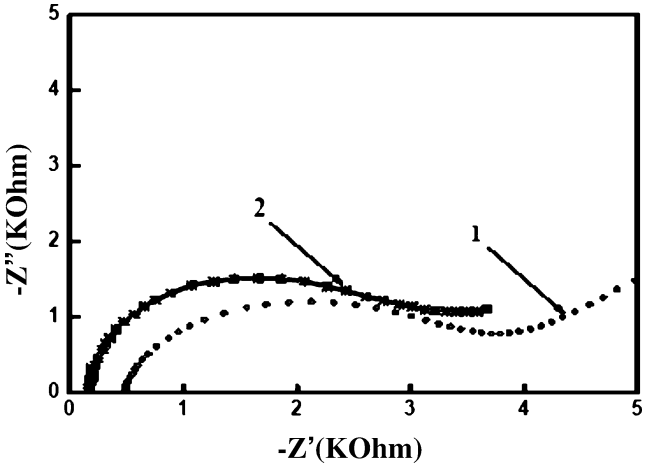

Fig. 7 Nyquist AC impedance frequency spectrum of different electrodes: (*1*) the bare gold electrode; (*2*) the dsDNA modified SAM/Au electrode. Frequency range: 100 kHz–0.05 Hz, potential step: 0.4–0.9 V, pulse width: 0.5 s

On the other hand, the AC current density can be represented by

$$i_0 = nFAk_f[S] \tag{8}$$

According to Eq. 8, we obtain

$$k_f = \frac{i_0}{nFA[S]} \tag{9}$$

where k_f (m/s) is the apparent reaction rate constant, A (m^2) is the electrode area, and $[S]$ ($mol \cdot L^{-1}$) is the concentration of the probe.

According to the above equations, the values of k_f (1.469×10^{-6} $m \cdot s^{-1}$) at the DNA-modified electrode can be obtained. Compared to the value of k_f (6.1876×10^{-4} $m \cdot s^{-1}$) obtained at the bare electrode, the value is drastically lowered, which means that DNA/Au forms an insulating film over the Au electrode for $Fe(CN)_6^{3-}$.

Imaging of surface-immobilized DNA electrode with SECM and AFM

SECM and AFM were used to characterize the modified Au surface. One of the applications of the SECM technique is to use the UME tip to obtain images of different substrate surfaces immersed in electrolyte solutions with about micrometer resolution. So, imaging of the obtained structure is performed in the conventional feedback mode of the SECM. The constant height mode is usually employed for reaction rate imaging. It offers a somewhat better resolution and is preferable for the imaging of mixed conductor/insulator surfaces. So, constant height images are obtained by rastering the tip across the substrate of interest in a fixed x–y plane above that of the substrate surface and recording the variations in the tip current. Variations in the current or potential at the tip during the scanning produce the images. By using this mode, metals, ionic crystals, and polymer films have been imaged.

Using the same medium and the same electrochemical reactions, we employed the SECM peculiarities to electrochemically visualize the bare and modified surfaces. Figure 8a–c shows the SECM images obtained from bare and modified gold electrodes using $Fe(CN)_6^{3-}$ as the electrochemical mediator. All the experiments were done at the same distance between tip and substrate (d=10 μm). The results are shown with reference to the normalized tip current (I_{norm}), which permits better comparisons between different experiments. When the electrode is nonmodified (Fig. 8a), the current is homogeneous in the entire explored surface, that is, the topography is regular. On the other hand, when the electrode is totally modified (Fig. 8c), a homogeneous current is also observed (a regular topography), but this current corresponds only to the tip current generation (I_{norm}=1), which represents a nonexistent feed-

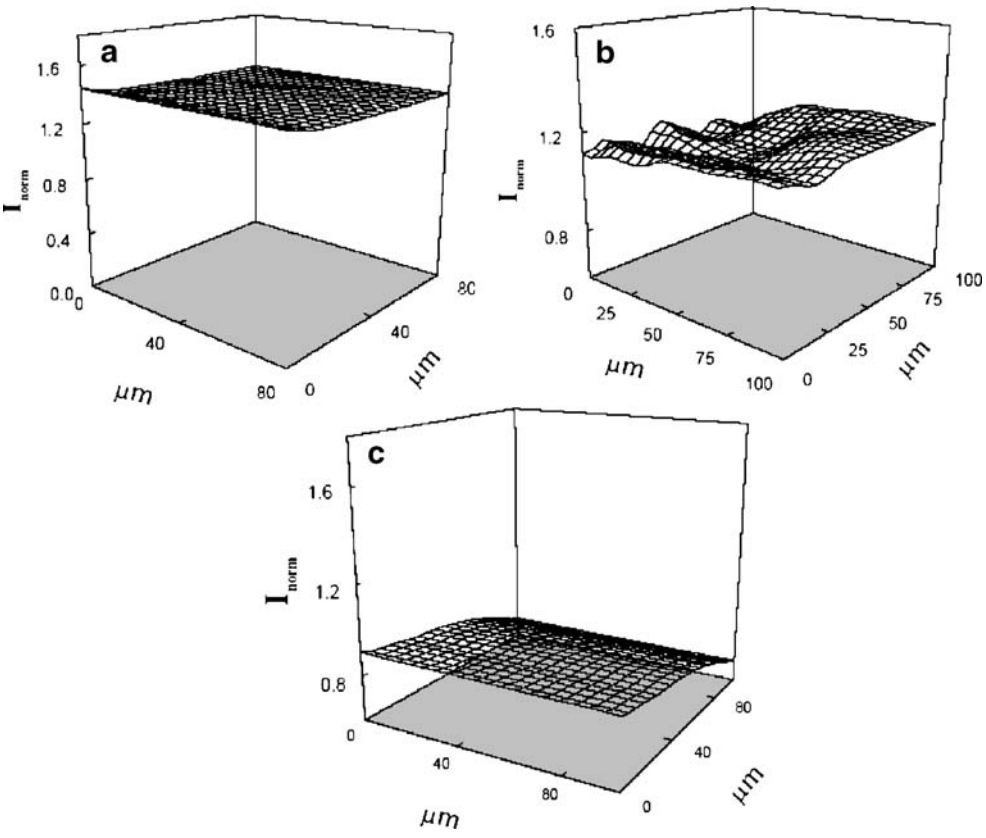

Fig. 8 SECM images: **a** the bare gold electrode; **b** the electrode partially modified with DNA (B=0.34); **c** the electrode totally modified with DNA. The tip was brought close to the surface at a rate of 1 μm·s^{-1} and positioned ca. 10 μm over each surface. The raster rate of the UME tip across the surface was 1 μm·s^{-1}

back with the substrate and is much lower, which shows that ET was effectively blocked. In the intermediate situation of covering (Fig. 8b), we can observe that the normalized current reaches an intermediate value when compared with the bare and totally modified electrode images. Moreover, the surface is not homogeneous. This fact gives a reliable explanation for the above results obtained (Fig. 5) with the feedback experiments at the partially modified electrode, wherein the approach curves evidence the differences in conductance. Clearly, it can be seen that the feedback current decreases over the monolayer film, as compared with the surrounding bare gold surface due to the additional diffusion barrier between the probe and the gold surface [30, 31]. The result not only reveals that the DNA can be well constructed on the Au electrode but also shows the surface information of the DNA as well.

AFM has been used extensively to obtain the nanoscopic structures of SAMs to a high degree of accuracy [32]. We have also used AFM to obtain the molecular packing structure of monolayer films. All the images presented are obtained at ambient temperatures in the contact mode. The bare surface clearly indicates that the surface is granular and evidently not modified significantly, which may be attributed to the polycrystallinity of the gold surface. Corresponding with the bare gold surface and the modified DNA–thiolglycolic acid surface, the AFM images of the Au–S surface show the complete coverage of the SAM over the grain boundaries of the Au surface and the formation of porous structures. These results confirm that the thiolglycolic acid forms a highly ordered monolayer on Au surfaces. In contrast, the strip-shaped structure of the DNA/Au SAM, which is similar to the DNA molecule, lies flat on the gold surface, indicating that the DNA molecule can be successfully assembled on the gold surface. Comparing the experimental data, it can be seen that the results obtained by SECM are quite consistent with those obtained by AFM.

Conclusion

In this work, we have carried out SECM, in situ AFM, and electrochemical AC impedance methods to study the formation of stable biochemically active monolayers. The DNA-modified gold electrode is characterized and can be used as a selective, conductive, or insulating substrate for CV and SECM experiments. By utilizing the feedback working mode, the SECM imaging of surface-confined DNA can be realized through the tip-induced reduction of $Fe(CN)_6^{3-}$. AFM and AC impedance methods were also used to study the surface progress. Taken together and based on experimental results, it can be inferred that DNA

duplexes had densely packed on the SAM/Au. Moreover, this is a very clear example wherein electrochemists can easily visualize the difference between electrochemistry at macroscopic (CV) and microscopic levels (SECM).

Acknowledgements This research was supported by a grant from the Natural Science Foundation of China (no: 20275031, 20335030), the Teaching and Research Award Program for Outstanding Young Teachers in Higher Education Institutions, The State Key Laboratory of Electroanalytical Chemistry, Changchun Institute of Applied Chemistry, Chinese Academy of Sciences.

References

1. Chen SM, Chen SV (2003) Electrochim Acta 48:513
2. Ma KS, Zhou H, Zoval J, Madou M (2006) Sens Actuators B Chem 114:58
3. Liu HH, Lu JL, Zhang M, Pang DW, Abruna HD (2003) J Electroanal Chem 544:93
4. Pang DW, Zhao YD, Fang PF, Cheng JK, Chen YY, Qi YP, Abruna HD (2004) J Electroanal Chem 567:339
5. Sonnenfeld R, Hansma PK (1986) Science 232(4747):211
6. Lustenberger P, Rohrer H, Christoph R, Sicgenthaler H (1988) J Electroanal Chem 243(1):225
7. Gu TT, Hasebe Y (2004) Anal Chim Acta 525:191
8. Christensen PA (1992) Chem Soc Rev 21(3):197
9. Wittstock G, Schuhmann W (1997) Electroanalysis 9:746
10. Wittstock G, Schuhmann W (1997) Anal Chem 69:5059
11. Shiku H, Tekeda T, Yamada H, Matsue T, Uchida I (1995) Anal Chem 67:312
12. Shiku H, Uchida I, Matsue T (1997) Langmuir 13:7239
13. Cai CX, Liu B, Mirkin MV, Frank HA, Rusling JF (2002) Anal Chem 74:114
14. Wittstock G (2001) Fresenius J Anal Chem 370:303
15. Liu B, Rotenberg SA, Mirkin MV (2000) Proc Natl Acad Sci U S A 97:9855
16. Bard AJ, Fan FRF, Pierce DT, Unwin PR, Wipf DO, Zhou F (1991) Science 254:68
17. Nassar AEF, Rusing JF, Nakashima N (1996) J Am Chem Soc 118:3043
18. Maeda M, Nakano K, Uchida S et al. (1994) Chem Lett 10:1805
19. Liu CY, Zhou XC, Jiang LP, Jian GY, Lu GH (2003) J Centr China Normal Univ Nat Sci 37(4):518
20. Kanayama N, Kanbara T, Kitano H (2000) J Phys Chem B 104:271
21. Zhang ZJ, Hou SF, Zhu ZH, Liu ZF (2000) Langmuir 16:537
22. Zhao YD, Pang DW, Hu S, Wang ZL, Cheng JK, Dai HP (1999) Tanata 49:751
23. Weisser M, Nelles G, Wohlfart P, Wenz G, Mittler-Neher S (1996) J Phys Chem 100:17893
24. Fukuda T, Maeda Y, Kitano H (1999) Langmuir 15:1887
25. Wittstock G, Schuhmann W (1997) Anal Chem 69:5059
26. Lu Z, Huang QJ, Rusling F (1997) Electroanal Chem 423:59
27. Laviron E (1979) Electroanal Chem 101:19
28. Tsionsky M, Bard AJ, Mirkin MV (1996) J Phys Chem 100:17881
29. Liu J, Li QW, Luo GA, Sun HW, Feng J (2002) J Instrum Anal 21:13
30. Turcu F, Schulte A, Hartwich G, Schuhmann W (2004) Angew Chem Int Ed Engl 43:3482
31. Turcn F, Schulte A, Hartwich G, Schuhmann W (2004) Biosens Bioelectron 20:925
32. Wen LX, Wu RC (2002) Eeschenazi Colloids Surf A Physicochem Eng Asp 157:197